Magnetic susceptibility, specific heat, and the spin-glass transition in $Hg_{1-x}Mn_xTe$

Shoichi Nagata, R. R. Galazka,* D. P. Mullin,† H. Akbarzadeh,
G. D. Khattak, J. K. Furdyna, P. H. Keesom
Department of Physics, Purdue University, West Lafayette, Indiana 47907
(Received 25 April 1980)

A systematic study of the low-dc-field magnetic susceptibility and the specific heat has been carried out on mixed $Hg_{1-x}Mn_xTe$ crystals, in the composition range $0 \leq x \leq 0.35$. The alloy with $x = 0.35$ showed spin-glass behavior below $T = 10.9$ K. At this Mn concentration the sample is a very poor conductor at low temperatures, so that the Ruderman-Kittel-Kasuya-Yosida (RKKY) mechanism cannot be responsible for the spin-glass transition. Also, since the Mn ions interact only antiferromagnetically, the observed spin-glass phase does not result from competition between ferro- and antiferromagnetic interaction. It must therefore be ascribed to the frustration of the antiferromagnetic interactions inherent in an fcc sublattice over which the Mn ions are distributed. For $x \leq 0.25$, the $Hg_{1-x}Mn_xTe$ samples remain paramagnetic down to 1 K. Experimental results for the specific heat and the susceptibility for $x < 0.1$ are discussed in terms of a cluster model which leads to an estimated value of the antiferromagnetic exchange constant $J/k \approx -0.7 \pm 0.3$ K. When a random distribution of Mn ions over the fcc sublattice is assumed, calculated values for the specific heat and the susceptibility differ substantially from the experimental results for the low Mn concentration. This therefore indicates that in real crystals the distribution of Mn ions is very different from random. To obtain agreement between calculated and experimental results, the number of single ions has to be reduced to less than 30% of the number corresponding to a purely random distribution, leading to the conclusion that the magnetic ions prefer to cluster rather than to remain isolated in $Hg_{1-x}Mn_xTe$. For HgTe, the Debye temperature Θ_D is 141 K at $T = 0$ K, and goes through an anomalously low minimum value of $\Theta_D = 77$ K at 7 K. A very small linear term in the low-temperature specific heat of HgTe gives an estimate of the electric charge carrier density in the 10^{18} cm^{-3} range.

I. INTRODUCTION

Solid solutions of HgTe and MnTe form ternary mixed crystals, $Hg_{1-x}Mn_xTe$, which belong to a group of materials known as semimagnetic semiconductors. These crystals are narrow-gap semiconductors with a variable energy gap, which depends on x and which can be either positive or zero. Recently the interest in these materials has been rapidly increasing, prompted by the fact that the presence of a magnetic constituent in the semiconductor lattice is expected to lead to new physical effects as a result of exchange interactions. In particular, the semiconducting properties of these materials, e.g., electrical transport,[1] microwave,[2] infrared and optical properties,[3] have been investigated extensively in the past several years. However, much less information is available on their magnetic and thermal properties, especially at low temperature, which motivated the present investigation. Our work on these solid solutions provides important information on the properties of a system of random magnetic ions.

Our measurements of the low-dc-field magnetic susceptibility and the specific heat of $Hg_{1-x}Mn_xTe$ covered the range of x between 0 and 0.35, for which the material forms a single crystallographic phase with the zinc-blende structure.[4] In this range of compositions the Mn ions randomly enter the zinc-blende structure of HgTe, where they replace the Hg ions and are thus distributed over an fcc sublattice. For $x > 0.36$, $Hg_{1-x}Mn_xTe$ tends to form more than one crystallographic phase, a situation unsuitable for the present investigation.

The extrinsic carriers in these materials are holes, with concentrations of the order of 10^{18} cm^{-3} or less. Hence localized magnetic moments are well defined. The ground state of the manganese in $Hg_{1-x}Mn_xTe$ is $^6S_{5/2}$. The energy splitting by the crystalline field is expected to be small because of the orbital singlet state, which will enable us to give a simple theoretical description for the experimental results.

We can distinguish two different regions of Mn concentration. For $x \leq 0.25$ the system remains paramagnetic for all temperatures. We believe that only finite clusters are present in this composition range. For $x = 0.35$ a spin-glass phase is observed

 ©1980 The American Physical Society

below 10.9 K, as might be expected for a crystal with randomly distributed magnetic ions. At low temperature the $x = 0.35$ crystal is a high-resistivity semiconductor, so that the Ruderman-Kittel-Kasuya-Yosida (RKKY) interactions between spins must be ruled out as the mechanisms responsible for the spin-glass behavior. Furthermore, since the Mn ions interact only antiferromagnetically, the observed spin-glass phase cannot be ascribed to the competition between ferro- and antiferromagnetic interactions. Instead the appearance of the spin-glass phase in this case is related to the fcc structure of Mn-ion sublattice, in which not all exchange energies for the magnetic bonds can be minimized simultaneously, so that the antiferromagnetic interaction of the spins is frustrated in the ground state. Theoretical predictions of a spin-glass phase due to this frustration mechanism were introduced by De Seze,[5] Toulouse,[6] Villain,[7] and by a computer simulation of Grest and Gabl.[8] Our experimental results are in qualitative agreement with these theoretical predictions, and appear to be clear evidence that frustration inherent in the lattice alone can lead to spin-glass properties. Similar spin-glass behavior was also observed in $Cd_{1-x}Mn_xTe$. The physical mechanisms underlying the appearance of a spin-glass phase are briefly summarized in Table I.[9–14]

Magnetic susceptibilities of $Hg_{1-x}Mn_xTe$ have already been measured by several investigators,[15–17] but these measurements were only done for a low Mn concentration range and in rather high magnetic fields. In a search of possible spin-glass formation a low magnetic field is essential, and therefore our measurements were performed in a field of 15 G.

For the low Mn concentration range, $x < 0.1$, previous workers[15,16] have tried to interpret their magnetic susceptibility results in terms of the sum of contributions from isolated Mn ions and ion pairs. We extended this calculation by also including three-ion clusters (triads). Calculations based on this cluster model will be compared with the experimental results for both the specific heat and the susceptibility. In our experiments specific heat is measured in several magnetic fields and its magnetic field dependence plays an important role in checking the applicability of our cluster model. The exchange constant J/k for antiferromagnetic coupling was evaluated in these calculations to be about -0.7 ± 0.3 K, which is substantially smaller than that obtained by previous workers.[1,15] But these previous investigators made use of the assumption that the Mn ions are randomly distributed over the fcc sublattice. This assumption, however, is not compatible with our experimental results. Our specific heat and susceptibility data show strong preference for cluster formation (pairs, triads, etc.), at the cost of isolated ions, a possibility which was already considered for this material by Andrianov *et al.*[16]

The present investigation has focused mainly on two aspects of the spin system of $Hg_{1-x}Mn_xTe$. The first is the spin-glass formation due to the frustration mechanism, which is different from the spin-glass model based on a competition between interactions of opposite sign. The second is the magnetic behavior for low Mn concentration, where it is possible to compare the experimental results with a simple cluster model, and to draw conclusions regarding the Mn-ion distribution in these materials.

TABLE I. Brief overview of spin-glasses for various interactions.

Spin-glass	Interaction	Example
Metal	RKKY, oscillatory	*Au*Fe[a]
		*Cu*Mn[b]
	Ferro- and antiferromagnetic, $+J$ and $-J$ competing	$Eu_xSr_{1-x}S$[c]
Insulator	Antiferromagnetic: $-J$, frustration due to lattice structure	$Cd_{1-x}Mn_xTe$[d]
		$Hg_{1-x}Mn_xTe$[e]
	Dipole-dipole interaction	
Amorphous system		$Gd_{0.37}Al_{0.63}$[f]
		$CoO \cdot Al_2O_3 \cdot SiO_2$[g]

[a]Reference 9.
[b]Reference 10.
[c]Reference 11.
[d]Reference 12.
[e]Present work.
[f]Reference 13.
[g]Reference 14.

II. EXPERIMENTAL

The $Hg_{1-x}Mn_xTe$ crystals were grown from appropriate quantities of Hg, Te, and Mn with purities of 99.9999999, 99.9999, and 99.99%, respectively, using a Bridgman method.[18] The starting materials were sealed in an evacuated thick-walled quartz ampule. This was placed in a vertical furnace and heated to 400 °C and held there for 24 hours to permit reaction between Hg and Te. The furnace temperature was then raised to 750 °C and maintained there for 48 hours to allow the manganese to dissolve and to form a homogeneous melt. The furnace was subsequently raised at a rate of 1.0 mm/h, moving a temperature gradient of about 1 °C/mm along the ampule. This procedure produced ingots that were largely monocrystalline. However, ingots with a high x value have an increased probability to become polycrystalline. Unless otherwise specified, all samples were subsequently annealed in a saturated Hg atmosphere at 240 °C to reduce the density of mercury vacancies.

The composition was determined by density measurements and by electron microprobe analysis. Crystals of $Hg_{1-x}Mn_xTe$ can be obtained for $x \leq 0.36$ in the zinc-blende crystallographic structure, but for $x > 0.36$, inclusions of $MnTe_2$ were found, so that the material was not suitable for our measurements.

Heat-capacity measurements were made using the standard heat-pulse technique in a conventional ^3He cryostat. The sample weight used in these measurements was typically 1 to 2 g. The susceptibilities χ were measured at a constant applied field of 15 G using a superconducting quantum interference device (rf SQUID). Typical samples used in the susceptibility measurement weighed 20 to 40 mg. Both experimental methods have been described in detail elsewhere.[19,20]

III. RESULTS AND DISCUSSION

A. Magnetic susceptibility

The results of magnetic susceptibility measurements for a wide range of compositions are shown in Fig. 1. The measurements were performed in a constant dc magnetic field of 15 G and the data were obtained from a continuous recording of the output of the rf SQUID. For $x = 0.35$ the susceptibility exhibits an anomaly at 10.9 K and below this temperature has a completely different character in comparison with samples of lower x.

As can be seen in the inset in Fig. 1, for $x = 0.35$ the value of the susceptibility $\chi = M/H$ is markedly dependent on the past magnetic history of the sample, i.e., whether the specimen had been cooled in the presence or in the absence of an applied field.

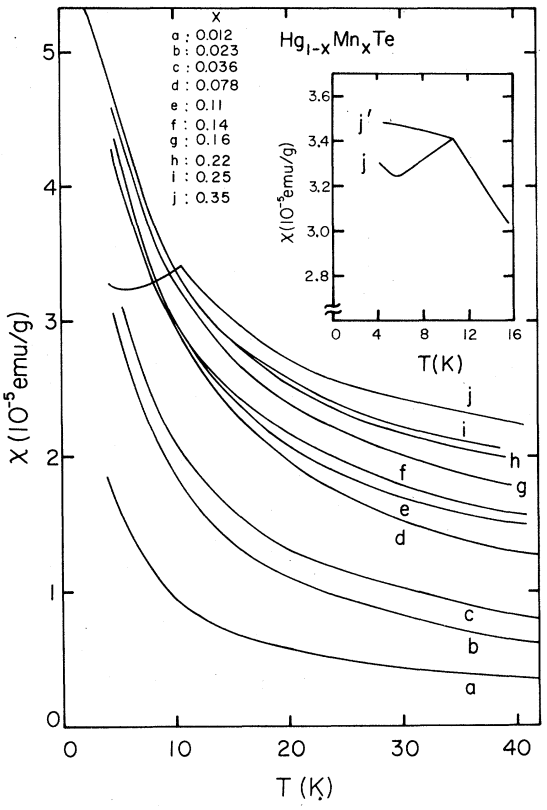

FIG. 1. Magnetic susceptibilities of $Hg_{1-x}Mn_xTe$ as a function of temperature. The inset gives the data for $x = 0.35$; labels j and j' indicate zero-field-cooled and field-cooled susceptibilities, respectively.

For the zero-field-cooled susceptibility, the sample was first cooled in a magnetic field of less than 0.05 G, and subsequently a magnetic field of 15 G was applied. A cusplike peak was then observed at the temperature $T_g = 10.9$ K. The field-cooled susceptibility (i.e., when the measuring field of 15 G had been applied *before* the sample was cooled below T_g) did not show a cusp at T_g. Within spans of 30 min no time dependence of the magnetization could be detected for the field-cooled and zero-field-cooled susceptibilities. This general behavior is similar to that for the metallic spin-glasses *Cu*Mn (Ref. 20) and *Au*Fe.[21] At the lowest temperatures, well below T_g, the susceptibility of the $x = 0.35$ sample again increased slightly with decreasing temperature, probably as a result of contributions from residual finite clusters, i.e., single ions, pairs, triads, etc. The susceptibilities for $x \leq 0.25$ increased monotonically down to 1.2 K and did not exhibit irreversible effects, in qualitative agreement with results obtained by previous workers.[16]

We interpret the anomaly observed for the $x = 0.35$ sample as being due to a spin-glass transition. The

crystal structure of this material is of the zinc-blende type, and this situation is favorable to the formation of the spin-glass phase as a consequence of the frustration mechanism already mentioned, since the magnetic ions form an fcc sublattice. The next-nearest-neighbor interaction J_{NNN} between magnetic ions is believed to be much smaller than the nearest-neighbor interaction J_{NN} for this structure, as was pointed out by Brumage *et al.*[22] on the basis of arguments about superexchange paths. (The existence of J_{NNN} would be important only if J_{NNN} were of opposite sign to J_{NN} and of comparable strength, since this could cause the system to have a spin-glass phase as a result of competition between these interactions, as was recently observed in $Eu_xSr_{1-x}S$.[11]) We therefore conclude that in this case the frustration mechanism is responsible for the spin-glass behavior in both the $Hg_{1-x}Mn_xTe$ measured here, as well as $Cd_{1-x}Mn_xTe$, studied by several of the present authors.[12]

The inverse susceptibilities versus temperature are plotted in Fig. 2. The high-temperature susceptibilities obey the Curie-Weiss law: $\chi = C/(T-\Theta)+\chi_0$, where χ_0 is temperature independent. The Weiss constant Θ vs Mn concentration is shown in Fig. 3. The downturn of these inverse susceptibilities can be accounted for by the presence of isolated magnetic ions or small clusters, which dominate the susceptibility contribution at low temperatures. In addition, this curvature is further enhanced by deviations from a random distribution of Mn ions on the fcc sublattice, which will be discussed later.

As pointed out earlier, from the susceptibility results we can distinguish two different Mn concen-

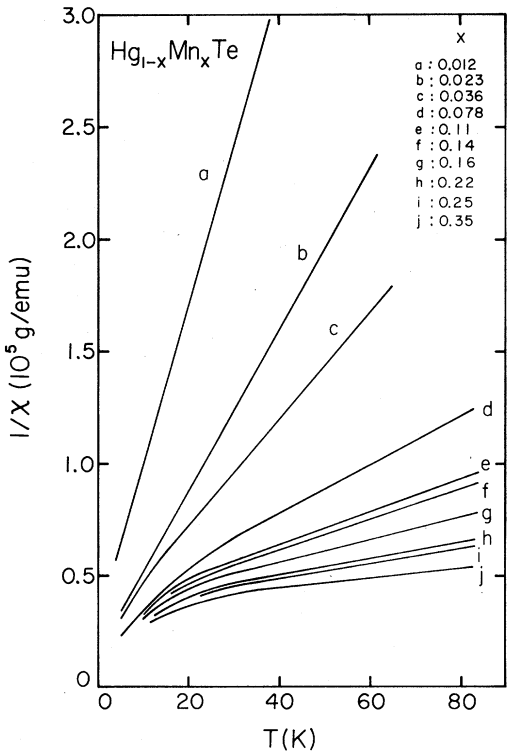

FIG. 2. Inverse susceptibilities vs temperature for $Hg_{1-x}Mn_xTe$.

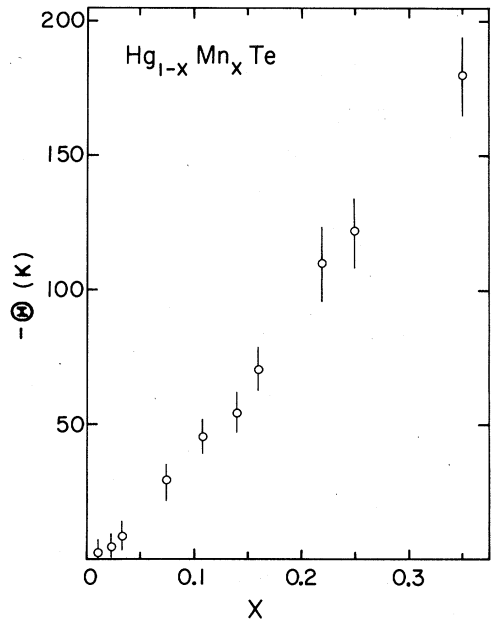

FIG. 3. Weiss constants $-\Theta$ as a function of Mn concentration x.

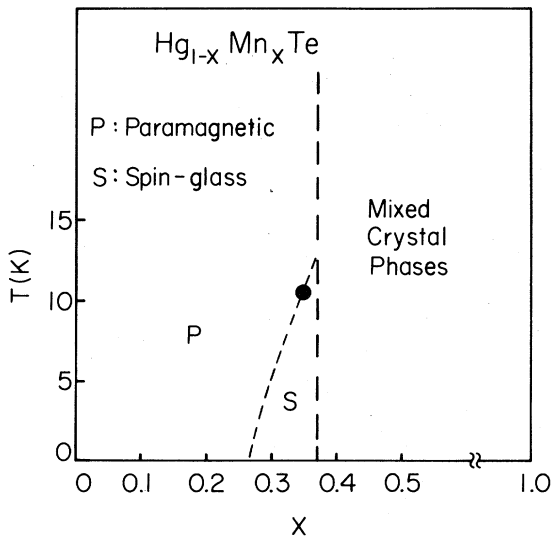

FIG. 4. Schematic phase diagram of $Hg_{1-x}Mn_xTe$ for temperature vs Mn concentration x. Regions P and S indicate paramagnetic and spin-glass phases, respectively.

tration regions. A very schematic phase diagram for the magnetic properties of $Hg_{1-x}Mn_xTe$ is presented in Fig. 4, which is qualitatively in agreement with the theoretical prediction of De Seze.[5] (In the diagram, the dashed line below 10 K should be regarded as indicating the lower limit of x corresponding to the spin-glass phase formation.) The system remains paramagnetic for $x \leq 0.25$ down to 1.2 K, where only small finite clusters of antiferromagnetically coupled spins are present. For $x > 0.25$ an infinite cluster (or perhaps a set of very large clusters) is responsible for the observed transition into the spin-glass phase.

B. Specific heat

1. HgTe

The results of specific heat measurements on an as-grown (not annealed) sample of HgTe are shown in Fig. 5. Below 1 K the specific heat can be represented by the expression

$$C = 42\,T + 1400\,T^3 \qquad (1)$$

in μJ/mole K. The T^3 term leads to the Debye temperature at $T = 0$ K of $\Theta_D = 141 \pm 2$ K, from the relation $C_L = (2)1944(T/\Theta_D)^3$ J/mole K, where C_L is the lattice contribution corresponding to six degrees of freedom of the HgTe molecule. This value of the Debye temperature is in excellent agreement with that obtained from measurements of elastic constants, $\Theta_D = 141 \pm 4$ K.[23]

Figure 6 shows the thermal Debye temperature Θ_D as a function of temperature. As compared with other solids, the temperature dependence of Θ_D is extremely large. It has a minimum at 7 K, where its value has decreased to 77 K, so that the specific heat at 7 K is approximately six times larger than predicted by an extrapolation of the low-temperature T^3 dependence. This anomalous behavior can be approximately understood on the basis of a neutron diffraction study by Kepa *et al.*[24] They found that two of the acoustic branches of the phonon dispersion relations have a maximum in the middle of the Brillouin zone and a local minimum at the X and L point of 1.5 meV. These very-short-wavelength acoustic modes start contributing already around 4 K and are the reason for the very low minimum in Θ_D. Replacing these short-wavelength modes by an Einstein mode is not sufficient to reproduce the experimental results, but a more detailed calculation based on the density of states of the lattice vibrations appears not to be warranted within the accuracy of the neutron data.

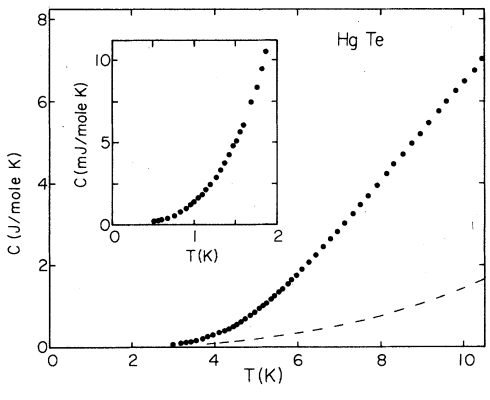

FIG. 5. Specific heat of HgTe vs temperature. The inset shows data at low temperatures. The dashed curve indicates the T^3 law with a Debye temperature of $\Theta_D = 141$ K at $T = 0$ K.

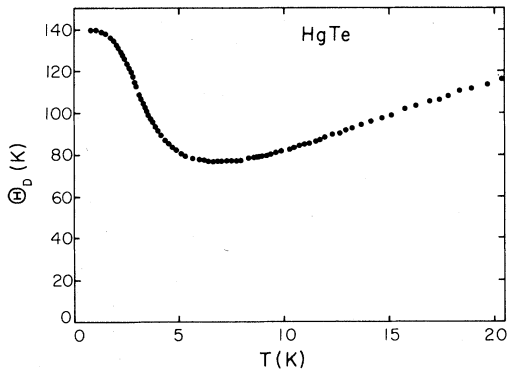

FIG. 6. Debye characteristic temperature for HgTe vs temperature.

The linear term in the specific heat in Eq. (1) is the electronic contribution and can be expressed by

$$C_e = \gamma T = 0.136\mu V_m^{2/3} n_a^{1/3} T \ , \qquad (2)$$

in mJ/mole K, where μ is the effective mass ratio of m^*/m for the charge carriers, V_m is the molar volume in cm^3, and n_a is the number of charge carriers per atom in the energy band. The effective mass ratios μ for electrons and holes are 0.02 and 0.5, respectively. Therefore, neglecting the electron contribution, it follows from Eq. (2) that the density of holes is 2.6×10^{18} cm^{-3}, which is a reasonable carrier density for as-grown HgTe.[25] This sample was remeasured after annealing at 240 °C in a saturated Hg atmosphere. This annealing decreased the density of holes, and their contribution to the specific heat was reduced by at least a factor of 10, while the lattice contribution was unchanged.

2. Specific heat of $Hg_{0.65}Mn_{0.35}Te$

Figure 7 shows the specific heat results for $x = 0.35$ in zero magnetic field, and in fields of 20 and 28 kG.

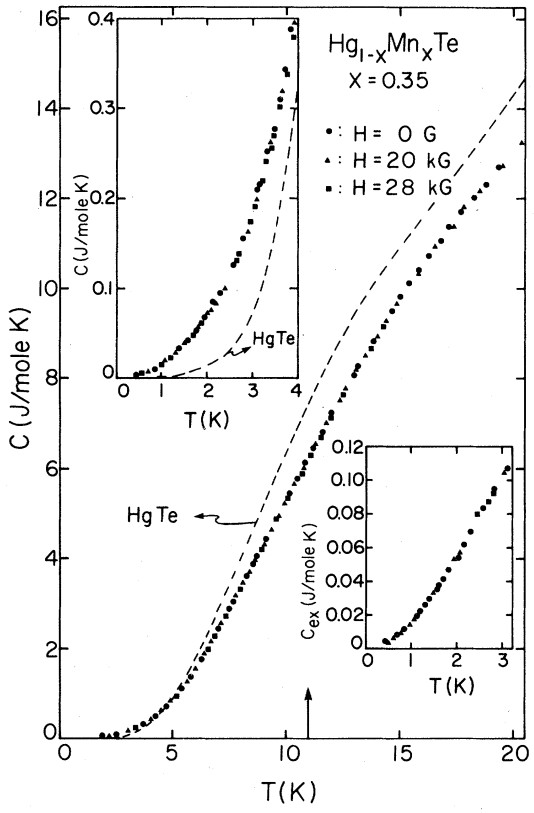

FIG. 7. Specific heat for the $x = 0.35$ sample as a function of temperature. The dashed curves indicate the specific heat of HgTe for comparison. The arrow marks $T_g = 10.9$ K, at which the susceptibility shows an anomaly. The upper inset shows the data in more detail for the low-temperature region. The lower inset gives the excess specific heat below 3K.

The susceptibility of this sample shows the characteristic cusp at the onset of the spin-glass phase at 10.9 K. This freezing temperature T_g is indicated by an arrow on the abscissa in Fig. 7. Note that the specific heat changes smoothly around T_g without any anomaly. It is also independent of the magnetic field up to 28 kG. For comparison, the specific heat of HgTe is also indicated by dashed lines. As can be seen, above 5 K the specific heat of the $x = 0.35$ sample is smaller than that of HgTe. This behavior is a consequence of substituting Mn ions for the much heavier Hg ions, which, in addition to introducing a magnetic contribution to the specific heat (our main interest), also introduces changes in the vibrational spectrum of the lattice. Specifically, this substitution shifts low-lying vibrational modes to much higher frequencies, which are not excited at low temperatures, and do not contribute to the specific heat. As a consequence of the uncertainty in the lattice specific heat due to the presence of manganese, the assessment of the magnetic contribution to the specific heat is then only possible at very low temperatures, where the lattice specific heat is small compared to the total specific heat C of the samples with manganese. This limits the usefulness of the definition of excess specific heat, $C_{ex} = C - C_{HgTe}$, for this sample to temperatures below 3 K. This excess specific heat C_{ex} is displayed in the lower inset of Fig. 7. It shows a linear temperature dependence, except below 1 K, a behavior already found in the case of the canonical spin-glass *Cu*Mn.[10]

3. *Specific heat of $Hg_{0.973}Mn_{0.027}Te$ and $Hg_{0.94}Mn_{0.06}Te$*

We studied these compositions as representative examples of the paramagnetic region. In Figs. 8

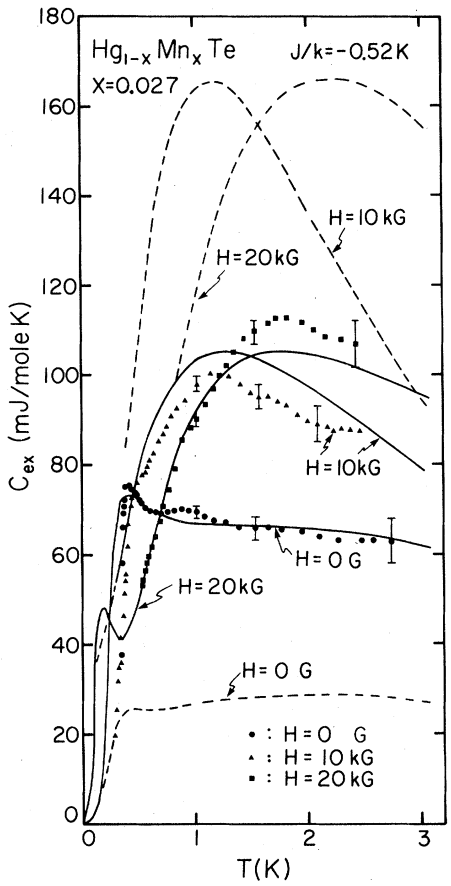

FIG. 8. Excess specific heat for the $x = 0.027$ sample as a function of temperature in zero field, and in magnetic fields of 10 and 20 kG. Dashed curves indicate specific heats calculated for a cluster model using the assumption of a random distribution of Mn ions. Solid curves show the calculated results for a distribution deviating strongly from a random distribution of Mn ions, as discussed in the text. Antiferromagnetic exchange constant $J/k = -0.52$ K is used for all calculations.

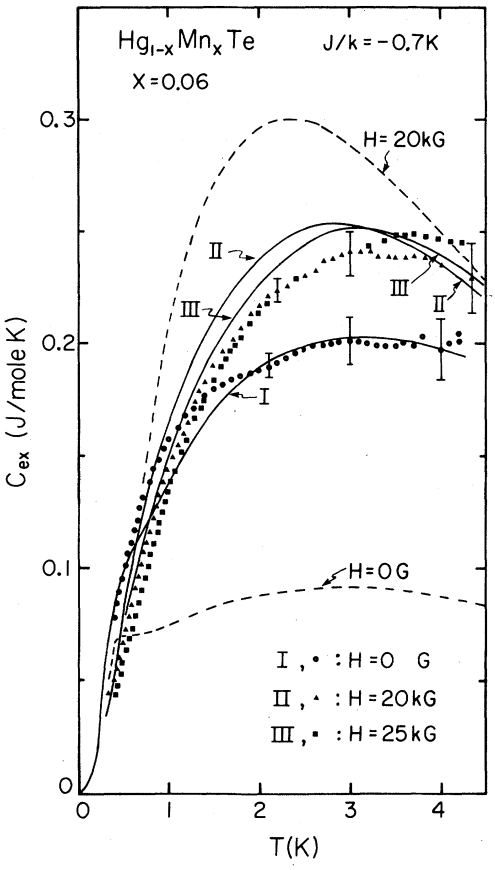

FIG. 9. Excess specific heat for the $x = 0.06$ sample vs temperature in fields of 0, 20, and 25 kG. Dashed curves give the calculated results assuming a random distribution of Mn ions. Solid curves indicate the results of a modified distribution, differing from random (see text).

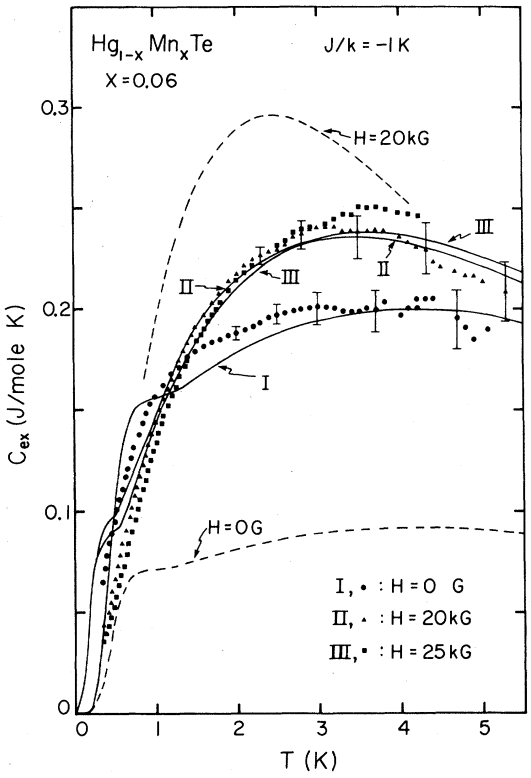

FIG. 10. Same experimental results as shown in Fig. 9. In this case, however, the exchange constant is taken as -1 K, and the contributions from each type of cluster are different from those employed in Fig. 9. Dashed curves indicate also the results of calculations for a random distribution.

through 10 we plot the excess specific heat (i.e., the difference between the specific heat of $Hg_{1-x}Mn_xTe$ and that of HgTe) for these paramagnetic compositions. The excess specific heat is markedly magnetic field dependent, in contrast to the specific heat of the $x = 0.35$ sample which showed the spin-glass behavior. Because of the low concentration of Mn ions involved, it was expected that these experimental results could be interpreted in terms of a simple cluster model which in turn should permit an evaluation of the exchange constant (see Sec. III C).

C. Exchange constant J

We analyze the experimental results for $x = 0.027$ and 0.06 and extract the exchange constant in terms of the following model. For these dilute compositions we assume a Heisenberg exchange interaction, taking place only between nearest-neighbor Mn ions

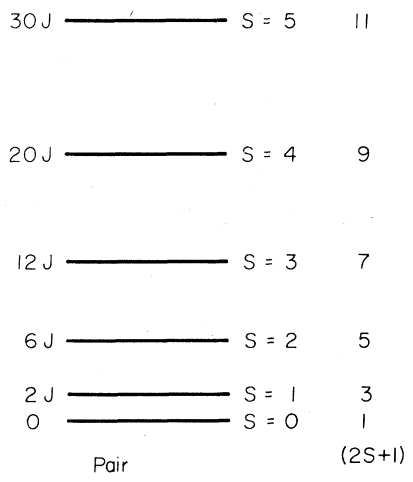

FIG. 11. Energy levels for a pair in the case of an antiferromagnetic coupling. The values of S characteristics for each level and the degeneracy $(2S + 1)$ are indicated.

TABLE II. Hamiltonians and their eigenvalues for various clusters, where $S_1=S_2=S_3=\frac{5}{2}$ and $g=2$.

Pair (P)	$\mathcal{H}=-2J(\vec{S}_1\cdot\vec{S}_2)-g\mu_B(S_1^z+S_2^z)H$ $\vec{S}_1=\vec{S}_2\equiv\vec{S}$ $E(S,M)=-J[S(S+1)-\frac{35}{2}]-g\mu_B mH$ $0\leq S\leq 5,\ \ \lvert m\rvert\leq S$
Closed triangle (T_c)	$\mathcal{H}=-2J[(\vec{S}_1\cdot\vec{S}_2)+(\vec{S}_2\cdot\vec{S}_3)+(\vec{S}_3\cdot\vec{S}_1)]$ $-g\mu_B(S_1^z+S_2^z+S_3^z)H$ $\vec{S}_1+\vec{S}_2+\vec{S}_3\equiv\vec{S},\ \ \vec{S}_1+\vec{S}_3=\vec{S}_a$ $E(S,M)=-J[S(S+1)-\frac{105}{4}]-g\mu_B mH$ $0\leq S_a\leq 5,\ \ \lvert S_a-\frac{5}{2}\rvert\leq S\leq S_a+\frac{5}{2},\ \ \lvert m\rvert\leq S$
Open triangle (T_o)	$\mathcal{H}=-2J[(\vec{S}_1\cdot\vec{S}_2)+(\vec{S}_2\cdot\vec{S}_3)]-g\mu_B(S_1^z+S_2^z+S_3^z)H$ $\vec{S}_1+\vec{S}_2+\vec{S}_3\equiv\vec{S},\ \ \vec{S}_1+\vec{S}_3=\vec{S}_a$ $E(S,S_a,M)=-J[S(S+1)-S_a(S_a+1)-\frac{35}{4}]-g\mu_B mH$ $0\leq S_a\leq 5,\ \ \lvert S_a-\frac{5}{2}\rvert\leq S\leq S_a+\frac{5}{2},\ \ \lvert m\rvert\leq S$

in the fcc sublattice. Additionally, we neglect the zero-field splitting of the energy by crystalline fields. In our nomenclature, we shall refer to any group of interacting Mn ions as a cluster. For convenience, this will also include the isolated single Mn ions as a type of "cluster." The cluster Hamiltonians can be readily written for two- and three-spin systems, and these are given in Table II. The energy levels of the pair and triad clusters for the case of antiferromagnetic coupling, obtained by using Kambe's method,[26] are shown in Figs. 11 through 13. In these figures J itself is defined to be a positive value.

It is necessary to define two types of clusters for three-spin systems. One is referred to as a "closed triangle," designated by T_c, in which each of the three magnetic ions is nearest neighbor to the other 2. The second type is called an "open triangle," labeled T_o, and represents three nearest-neighbor Mn ions located on an open string. We then write the susceptibility and the specific heat in the form

$$\chi=\sum_i N_i\chi_i\ , \tag{3}$$

$$C=\sum_i N_i C_i\ , \tag{4}$$

where χ_i and C_i are the contribution from each cluster (including single ions), and N_i is the number of the ith cluster. The susceptibility and the specific heat for each cluster are given by

$$\chi_i=\frac{g^2\mu_B^2}{3kT}\ \frac{\sum_s S(S+1)(2S+1)\exp(-\epsilon_s/kT)}{\sum_s (2S+1)\exp(-\epsilon_s/kT)}\ , \tag{5}$$

$$C_i=\frac{\partial}{\partial T}\ \frac{\sum_s E_s\exp(-E_s/kT)}{\sum_s \exp(-E_s/kT)}\ , \tag{6}$$

where μ_B is the Bohr magneton, k is the Boltzmann constant, g is the Landé g factor (we used $g=2$),[2,27] and ϵ_s is the energy when magnetic field $H=0$, given in Figs. 11 through 13. In the presence of a magnetic field, E_s is defined by $E_s=\epsilon_s-g\mu_B mH$, where m is the magnetic quantum number. In the process of summation care has to be taken to account for degeneracy, which is indicated by W in Fig. 12 for

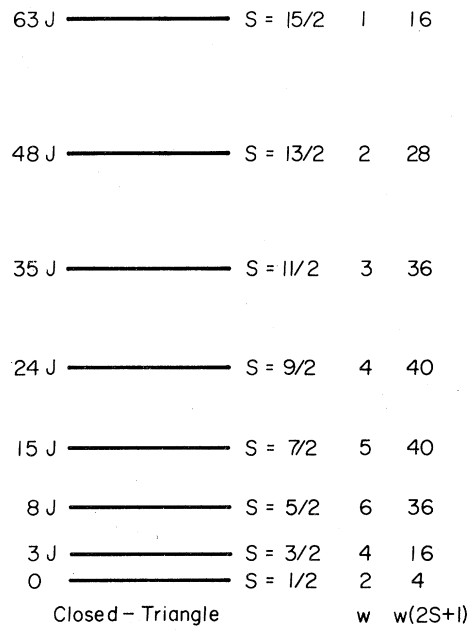

FIG. 12. Energy levels for a closed triangle. The value of W indicates the degeneracy of each level.

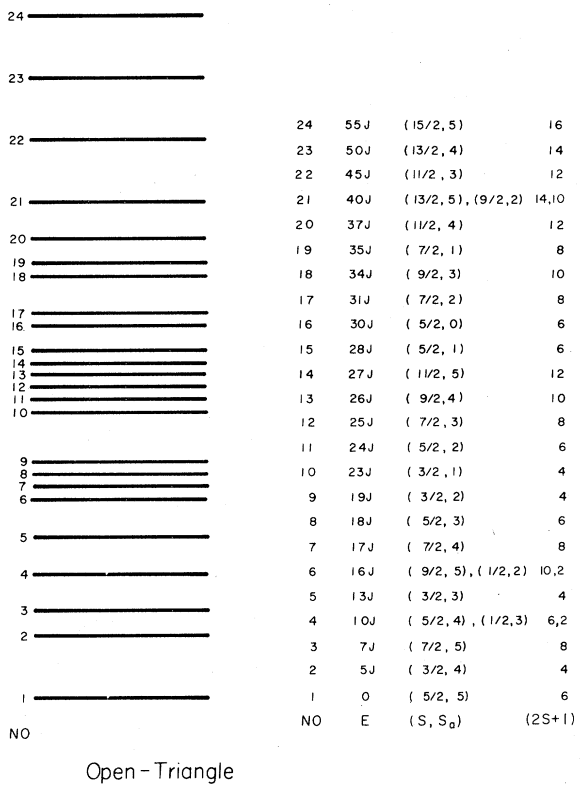

24	55J	(15/2, 5)	16
23	50J	(13/2, 4)	14
22	45J	(11/2, 3)	12
21	40J	(13/2, 5), (9/2, 2)	14,10
20	37J	(11/2, 4)	12
19	35J	(7/2, 1)	8
18	34J	(9/2, 3)	10
17	31J	(7/2, 2)	8
16	30J	(5/2, 0)	6
15	28J	(5/2, 1)	6
14	27J	(11/2, 5)	12
13	26J	(9/2, 4)	10
12	25J	(7/2, 3)	8
11	24J	(5/2, 2)	6
10	23J	(3/2, 1)	4
9	19J	(3/2, 2)	4
8	18J	(5/2, 3)	6
7	17J	(7/2, 4)	8
6	16J	(9/2, 5), (11/2, 2)	10,2
5	13J	(3/2, 3)	4
4	10J	(5/2, 4), (11/2, 3)	6,2
3	7J	(7/2, 5)	8
2	5J	(3/2, 4)	4
1	0	(5/2, 5)	6
NO	E	(S, S_a)	(2S+1)

FIG. 13. Energy levels for an open triangle. The values of S and S_a, characteristic for each level, are shown in parentheses. The value of $(2S+1)$ is also shown.

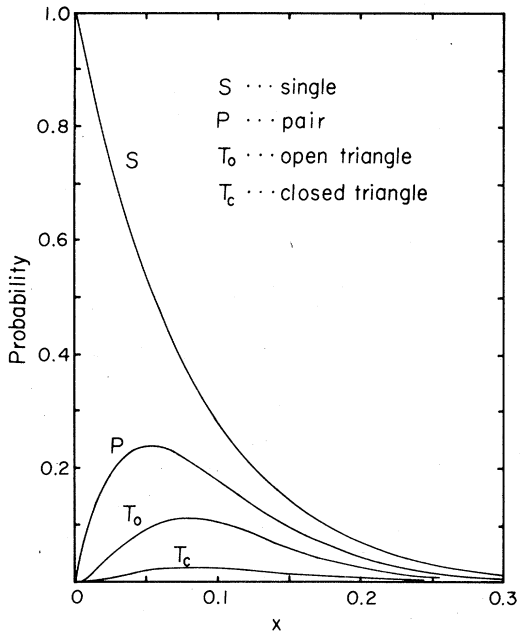

FIG. 14. Probability of finding a given magnetic ion in a particular type of cluster, i.e., single (S), pair (P), open triangle (T_o), or closed triangle (T_c). A random distribution of ions over an fcc lattice is assumed.

closed triangles, and for open triangles by the two different sets of (S,S_a) on the same line in Fig. 13.

To calculate the magnetic specific heat, the distribution of the Mn ions over the different clusters has to be known. It is most natural to assume that the Mn ions together with the Hg ions are distributed randomly over the sites of the fcc sublattice. The calculated probabilities for isolated ions, pairs, and triads in such a random distribution are shown in Fig. 14 as a function of Mn concentration x (see Appendix A). With this assumption, only the Heisenberg exchange parameter J is adjustable. In zero magnetic field the isolated ions do not contribute to the specific heat, since the zero-field splitting of the ground state is negligible, so that only the clusters with $n > 1$ contribute. The temperature dependence of this zero-field specific heat is a function of $kT/|J|$. A sample calculation for this case is considered in Appendix B. In Figs. 8 and 9 we also show (in dashed curves) the results for this random distribution calculated with appropriate J values. It can be seen that the theoretical predictions do not agree at all with the experimental results, the magnitude of the specific heat differing substantially from the predictions of the model. The $x = 0.027$ sample shows especially striking differences. Its measured zero-field specific heat shows a pronounced peak at 0.42 K, and the whole observed temperature dependence of the specific heat suggests that the pairs are the dominant contributors to the specific heat (see Appendix B). The location of the observed maximum gives the value for $J/k = -0.52$ K. The results measured in magnetic fields also lead to the conclusion that the assumption of a random distribution of Mn ions over the fcc sublattice is not tenable.

Once the assumption of a random distribution is rejected, a Pandora's box of possibilities is opened, since then the probabilities of finding a Mn ion to be a single isolated ion, or a member of a pair or a triad, become adjustable parameters. To distinguish this situation from the random distribution model, we shall call it the "modified distribution A." Using this modification, we first deduce from the zero-field specific heat the probabilities for pair and triad distributions. The magnetic field data then lead to the probability of the single ion distribution. For the $x = 0.027$ sample the exchange parameter J follows directly from the temperature corresponding to the maximum in the specific heat, but since the $x = 0.06$ sample did not show the same characteristics, J was also treated as an adjustable parameter. The results of these fitting procedures are shown in Figs. 8 and 9 as solid curves.

TABLE III. Probability distribution: the probability of finding a given Mn ion in a given cluster type of single (S), pair (P), closed triangle (T_c) and open triangle (T_o). Using these distributions, the calculated results are shown in Figs. 8 to 10.

	$x=0.027$		$x=0.06$		
	Random distribution	Modified distribution (A)	Random distribution	Modified distribution (A)	(B) ($R=0.1$)
Single (S)	0.720	0.23	0.476	0.02	0.048
Pair (P)	0.198	0.59	0.236	0.30	0.515
Closed triangle (T_c)	0.0096	0	0.022	0.10	0.048
Open triangle (T_o)	0.048	0	0.105	0.40	0.228

The data of the $x=0.06$ sample was also analyzed via another approach, the "modified distribution B." As argued above, the probability of single ions has to be reduced by a factor R (<1). In this modification the "lost" single ions are redistributed over the pairs and triads proportional to the probability of pairs and triads calculated for the random distribution. Figure 10 shows the result of this attempt. In Table III are displayed the results of a random distribution and of the modified distributions A and B. Obviously the modified distributions produce better agreement with the experimental data, but the agreement is still rather poor. We will return to this point shortly.

The susceptibility results provide an additional check on this model, although it is rather less sensitive to the exchange parameter J than the specific heat. The solid curves in Fig. 15 give the inverse of the experimental susceptibilities for three samples: $x=0.012$, 0.023, and 0.078. The dashed curves, representing the theoretical susceptibilities calculated assuming a random distribution, are well below the experimental curves. Contribution by clusters with $n>3$, neglected in the calculation, would lead to still lower inverse susceptibilities. Thus the susceptibility results lead to the same conclusion as the specific heat: the number of isolated ions has to be reduced. It should be remarked that if only a random distribution is assumed, then to fit the susceptibility data the value of J has to be increased drastically (see, e.g., curve g in Fig. 15). Such a large value of J would not be compatible with the specific heat results.

Finally, we point out some limitations of the simple cluster model and its modifications employed in the present discussion. (i) The model assumes a homogeneous distribution of Mn ions throughout the sample. Composition analysis by an electron microprobe, however, showed considerable local deviations in the Mn ion distribution. (ii) We neglect the contribution to the specific heat and the susceptibility by clusters with $n>3$ in the model. This is a good approximation for small x, but the neglect of large clusters should become increasingly serious as x increases (see Fig. 14). (iii) We also neglect the existence of a next-nearest-neighbor interaction. This interaction is small, but it may affect the energy scheme.[28] In particular, if this interaction affects the energy of the first excited state even slightly, the

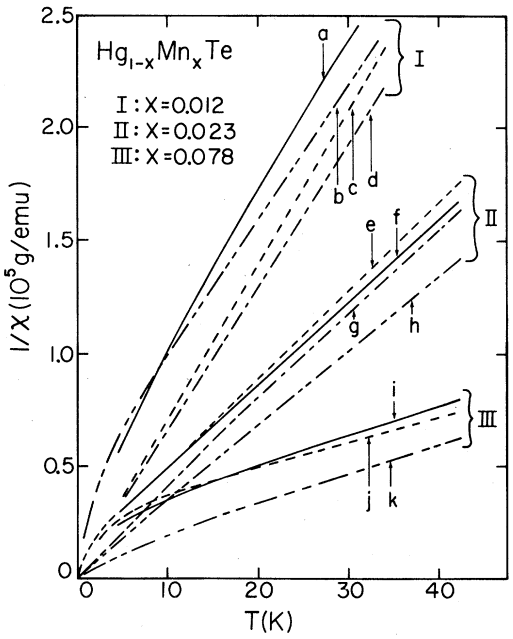

FIG. 15. Inverse susceptibilities vs temperature for $x=0.012$, 0.023, and 0.078. Solid curves a, f, and i indicate the experimental results, respectively. Results of several calculations are given for comparison, as follows: curve b $J/k=-1$ K, reduction factor $R=0.3$; curve c $J/k=-6$ K, random distribution; curve d $J/k=1$ K, random distribution; curve e $J/k=-0.52$ K, the same distribution as was obtained from the fitting of the specific heats in Fig. 8; curve g $J/k=-6$ K, random distribution; curve h $J/k=-0.52$ K, random distribution; curve j $J/k=-2$ K, reduction factor $R=0.1$; and curve k $J/k=-2$ K, random distribution.

TABLE IV. Summary of the distributions of ions over an fcc lattice. The concentration of ions is x and the number of lattice sites is N.

Cluster type	Probability of an ion to be in a type of cluster	Number of ions belonging to a given cluster type	Number of clusters
Single (S)	$(1-x)^{12}$	$Nx(1-x)^{12}$	$Nx(1-x)^{12}$
Pair (P)	$12x(1-x)^{18}$	$12Nx^2(1-x)^{18}$	$6Nx^2(1-x)^{18}$
Open triangle (T_o)	$18x^2(1-x)^{23}[5(1-x)+2]$	$18Nx^3(1-x)^{23}[5(1-x)+2]$	$6Nx^3(1-x)^{23}[5(1-x)+2]$
Closed triangle (T_c)	$24x^2(1-x)^{22}$	$24Nx^3(1-x)^{22}$	$8Nx^3(1-x)^{22}$

specific heat at low temperature can be changed markedly. (iv) Since the ionic radii of Hg and Mn are quite different (1.10 and 0.80 Å, respectively), it is to be expected that the exchange parameter depends on the number of Mn ions in a given cluster. This would lead to a value of J which depends on n. (v) The additional so-called biquadratic exchange interaction terms of the form $J'(\vec{S}_i \cdot \vec{S}_j)^2$ and more complicated interactions, neglected in the present analysis, may give a more realistic representation of the spin system, as has been discussed by many investigators.[29–32]

Since the deviation from a random distribution leads to strong effects and complexities of its own, none of the above points were taken into account. It is satisfying that the experimental results can at least qualitatively be reproduced using the modified distributions. The difference between experimental results and theoretical calculations indicates that the neglected effects probably have a measurable influence on the specific heat and the susceptibility, and this point should perhaps be borne in mind for future investigations.

IV. CONCLUDING REMARKS

The low-temperature specific heat and the magnetic susceptibility of $Hg_{1-x}Mn_xTe$ for several representative values of x have been measured. The results of this work can be summarized as follows. The thermal and magnetic properties can be understood on the basis of well-defined localized magnetic moments which are distributed over an fcc sublattice in the zinc-blende structure. In this structure the next-nearest-neighbor interaction between the magnetic ions is not strong enough to compare with the nearest-neighbor interaction. Under these conditions, it was pointed out by De Seze[5] that a spin-glass phase due to the frustration of the antiferromagnetic interaction becomes favorable at low temperatures. We observe this phase transition in $Hg_{1-x}Mn_xTe$ when $x = 0.35$. The susceptibility for this composition shows a cusp at $T_g = 10.9$ K and an irreversible behavior below T_g. The specific heat was linearly proportional to the temperature (except for very low temperatures), did not show any anomaly at T_g, and was not magnetic field dependent within the experimental accuracy.

For $x \leq 0.25$ the $Hg_{1-x}Mn_xTe$ crystals are paramagnetic at all temperatures, and only finite clusters exist, without magnetic long-range order. In this region of compositions the susceptibilities increase monotonically with decreasing temperature, and the specific heats exhibit broad maxima at low temperatures and are magnetic field dependent. A cluster model calculation was carried out for these low Mn concentration samples, and the antiferromagnetic exchange constant was estimated to be $J/k = -0.7 \pm 0.3$ K. This differs significantly from the estimates by previous investigators.[1,15] The experimental data of the specific heat and the susceptibility could not be explained in terms of a random distribution on Mn ions over the fcc sublattice. We conclude on this

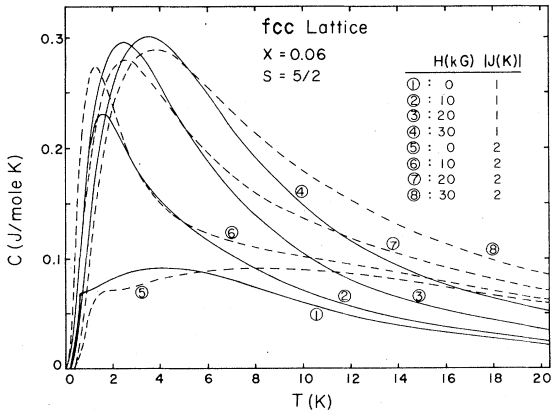

FIG. 16. Calculated specific heat vs temperature, for several values of the magnetic field and the exchange constant. The solid and dashed curves are for $J/k = -1$ and -2 K, respectively. A random distribution is assumed.

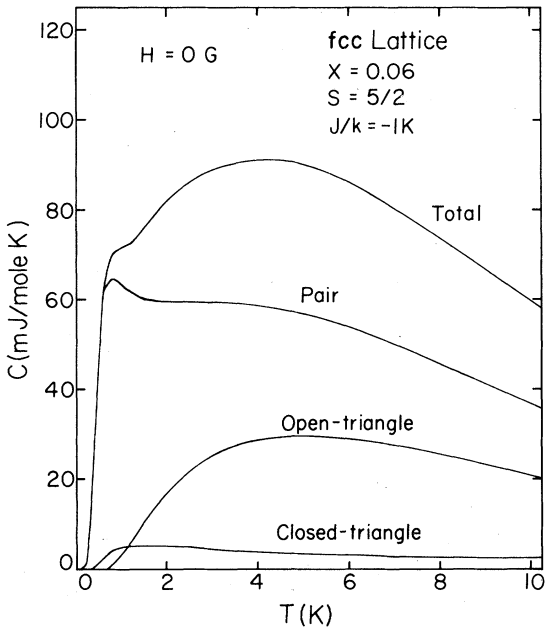

FIG. 17. Contributions by various cluster types to the specific heat in zero magnetic field, assuming a random distribution.

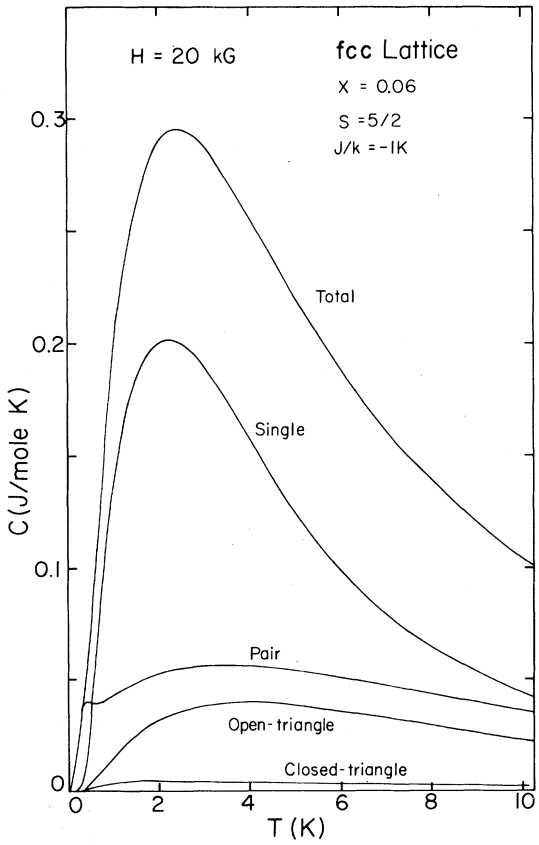

FIG. 18. Contributions by various cluster types to the specific heat in 20 kG, assuming a random distribution.

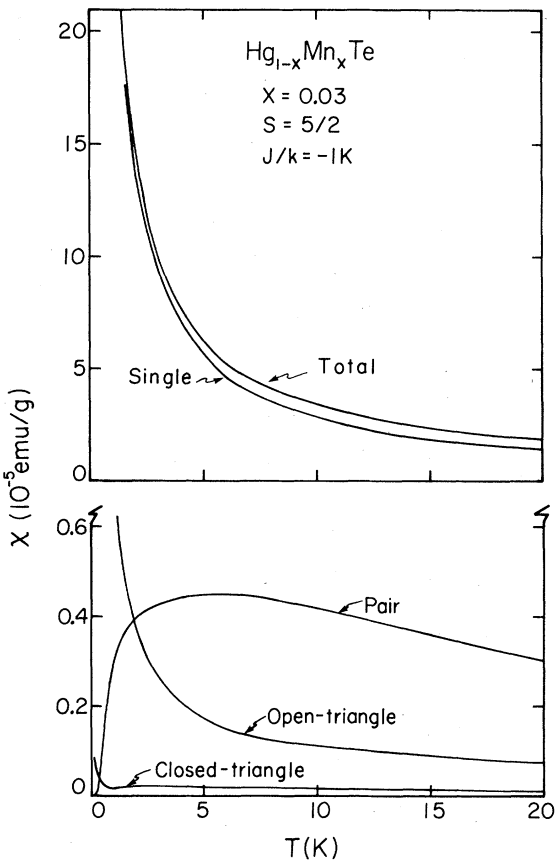

FIG. 19. Contribution to the susceptibility from each type of cluster in the case of a random distribution.

basis that the random distribution of Mn ions is incorrect for the $Hg_{1-x}Mn_xTe$, and that the individual magnetic ions in this material have a tendency toward cluster formation.

ACKNOWLEDGMENTS

The authors are grateful to Professor G. S. Grest for stimulating and encouraging discussions. This work was supported by the National Science Foundation MRL Grant No. DMR77-23798.

APPENDIX A

Table IV summarizes the distribution between different cluster types in a random distribution of ions over an fcc lattice, following Ref. 33. The number of lattice sites is N, while the concentration of ions distributed randomly over these sites is x. If an ion has no other ion as a nearest neighbor, it is said to be single. When two ions are nearest neighbors to each other, they are called a pair. For three ions in a clus-

ter we distinguish a closed triangle when each ion has two nearest neighbors, or an open triangle when only one of the three ions has two nearest neighbors. The probability distribution indicates the probability that a given ion belongs to a particular type of cluster. The probability as a function of Mn concentration x for different clusters is shown in Fig. 14.

APPENDIX B

As an illustration, the results of specific heat calculations are shown in Fig. 16 for two values of the exchange constant J and for several magnetic fields. In zero-field the temperature dependence of the specific heat is a function of $kT/|J|$, and this feature makes the zero-field specific heat much more sensitive to the exchange constant in comparison with results in finite magnetic fields, as can be seen from the figure. These calculations are based on the assumption of a random distribution of Mn ions. Using the same assumption, the specific heat contributions from the different clusters were calculated for $J/k = -1$ K and $x = 0.06$ in zero field (see Fig. 17) and in field of 20 kG (see Fig. 18). Figure 19 shows the contributions of the various clusters to the gram susceptibility of $Hg_{1-x}Mn_xTe$ calculated for the following parameters: $x = 0.03$, $g = 2$, $S = \frac{5}{2}$, and $J/k = -1$ K.

---

*On leave from Institute of Physics, Polish Academy of Sciences, Warsaw, Poland.
†Present address: Naval Ocean Systems Center, San Diego, Calif. 92152.

[1]M. Jaczynski, J. Kossut, and R. R. Galazka, Phys. Status Solidi (b) 88, 73 (1978).
[2]R. T. Holm and J. K. Furdyna, Phys. Rev. B 15, 844 (1977).
[3]G. Bastard, C. Rigaux, Y. Guldner, J. Mycielski, and A. Mycielski, J. Phys. (Paris) 39, 87 (1978).
[4]R. T. Delves and B. Lewis, J. Phys. Chem. Solids 24, 549 (1963).
[5]L. De Seze, J. Phys. C 10, L353 (1977).
[6]G. Toulouse, Commun. Phys. (G.B.) 2, 115 (1977).
[7]J. Villain, Z. Phys. B 33, 31 (1979).
[8]G. S. Grest and E. F. Gabl, Phys. Rev. Lett. 43, 1182 (1979).
[9]V. Cannella and J. A. Mydosh, Phys. Rev. B 6, 4220 (1972).
[10]L. E. Wenger and P. H. Keesom, Phys. Rev. B 13, 4053 (1976).
[11]H. Maletta and W. Felsch, Phys. Rev. B 20, 1245 (1979).
[12]R. R. Galazka, S. Nagata, and P. H. Keesom, Phys. Rev. B 22, 3344 (1980) (following paper).
[13]T. Mizoguchi, T. R. McGuire, S. Kirkpatrick, and R. J. Gambino, Phys. Rev. Lett. 38, 89 (1977).
[14]R. A. Verhelst, R. W. Kline, A. M. de Graaf, and H. O. Hooper, Phys. Rev. B 11, 4427 (1975).
[15]S. Savage, J. J. Rhyne, R. Holm, J. R. Cullen, C. E. Carroll, and E. P. Wohlfarth, Phys. Status Solidi (b) 58, 685 (1973).
[16]D. G. Andrianov, F. A. Gimel'farb, P. I. Kushnir, I. E. Lopatinskii, M. V. Pashkovskii, A. S. Savel'ev, and V. I. Fistul', Sov. Phys. Semicond. 66, (1976).
[17]U. Sondermann and E. Vogt, Physica (Utrecht) 86–88B+C, 419 (1977).
[18]D. P. Mullin, Ph.D. thesis (Purdue University, 1980) (unpublished).
[19]G. M. Seidel and P. H. Keesom, Rev. Sci. Instrum. 29, 606 (1958).
[20]S. Nagata, P. H. Keesom, and H. R. Harrison, Phys. Rev. B 19, 1633 (1979).
[21]J. L. Tholence and R. Tournier, J. Phys. (Paris) 35, C4-229 (1974).
[22]W. H. Brumage, C. R. Yarger, and C. C. Lin, Phys. Rev. A 133, 765 (1964).
[23]T. Alper and G. A. Saunders, J. Phys. Chem. Solids 28, 1637 (1967).
[24]H. Kepa, W. Gebicki, and T. Giebultowicz (private communication).
[25]K. Szlenk, Phys. Status Solidi (b) 95, 445 (1979).
[26]K. Kambe, J. Phys. Soc. Jpn. 5, 48 (1950).
[27]R. T. Holm and J. K. Furdyna, Solid State Commun. 15, 1459 (1974).
[28]See, for example, O. Okada, J. Phys. Soc. Jpn. 48, 391 (1980).
[29]E. A. Harris and J. Owen, Phys. Rev. Lett. 11, 9 (1963).
[30]D. S. Rodbell, I. S. Jacobs, and J. Owen, Phys. Rev. Lett. 11, 10 (1963).
[31]N. L. Huang, and R. Orbach, Phys. Rev. Lett. 12, 275 (1964).
[32]T. Iwashita and N. Uryu, J. Phys. Soc. Jpn. 36, 48 (1974), and references therein.
[33]R. E. Behringer, J. Chem. Phys. 29, 537 (1958).